Iraqi National Journal of Chemistry

Journal homepage:
http://iqnjc.com/Default.aspx

Preparation and Characterization of Ni (II) Complex using a New Schiff base-Azo Reagent (HTYPIM)

Muntadhar Adnan Rahman[1*], Muneer A. Al-Da'amy[2]

[1]*Chemistry Department, College of Education for Pure Science, University of Kerbala, Najaf, Iraq*
[2]*Chemistry Department, College of Science, University of Kerbala, Kerbala, Iraq *For Corresponding author: Email address: montather.a@s.uokerbala.edu.iq (Muntadhar Adnan Rahman)*

Abstract:

In this study, a new organic azo-Schiff base ligand was prepared in two steps: condensation and diazotization. This ligand is used to react with the copper(II) ion to form a copper complex and to determine small amounts of it. The prepared ligand and complex were characterized by UV-Vis, FT-IR, and 1H NMR spectra, and the molar electrical conductivity of the complex was also measured. Ion copper (II) was determined by a rapid, sensitive, simple and cheap spectrophotometric method, the copper compound has a molar absorbance of (1.764×10^{5}) L.mo1^{-1}.cm^{-1}, a Sandel sensitivity of (3.327×10^{-4}) µg.cm^{-2}, and a maximum absorbance of (417) nm, with a limit of detection of (0.0075) µg.mL^{-1} and a limit of quantitation of (0.025) µg.mL^{-1}, the metal concentration obeys Beer's law within the range (0.05-1.25) µg.mL^{-1} with a correlation coefficient value of (0.9996) indicating the degree of linearity of the standard calibration for copper. In the complex, the molar ratio of the metal to the ligand was [1:2]. The results indicate that the complex has a high stability constant of 4.4546×10^8 (mol·L^-1), and these results show that this method was more sensitive, more precise, and more accurate, as evidenced by the calculated (Re, Erel, R.S.D) (%).

Keywords: Schiff base, Azo methene, 2-Aminothiazole, Ni (II) complex

1. Introduction:

Nickel (Ni) is considered one of the important transition elements in the periodic table, with an atomic number of 28 and an atomic weight of approximately 58.69 g/mol, nickel is characterized by its electronic configuration ($[Ar]^{18}3d^84s^2$), Which gives it the ability to form various coordination complexes due to the presence of electrons in the d orbital [1,2], In terms of abundance the percentage of nickel in the Earth's crust is about 84 parts per million, making it the twenty-fourth most abundant element [3], nickel is commonly found in nature in the form of sulfide minerals such as (Pentlandite) and oxides such as (Garnierite), and it is extracted in large quantities from deposits in Canada, Russia, and Australia [4], nickel is a silver-colored shiny metal, characterized by high hardness and durability, with a density of about 8.90 g/cm³, a melting point of (1455) C°, and a boiling point close to (2913)C° [5]. nickel also exhibits magnetic properties, as it is one of the magnetic metals alongside iron and cobalt, making it important in electronic and magnetic applications [6], Nickel exhibits several oxidation states, the most important of which are +2, +3, and +4, in addition to less common states such as +1 and 0 in some organometallic complexes [7], the most common and stable state is +2, where nickel (II) forms stable coordination complexes with a wide range of ligands such as amines and phosphines [8], industrially, nickel is mainly used in the production of corrosion- and heat-resistant alloys such as stainless steel. It is also used in the manufacture of rechargeable batteries and electroplating [9]. In coordination chemistry, nickel is characterized by its ability to form stable complexes with a wide range of ligands. These complexes exhibit diverse electronic and magnetic properties due to variations in ligand field strength, making them important in spectroscopic studies and chemical catalysis [10].

2. Methodology:

2.1- Materials:

All solvents and chemical Reagents used in this study have high purity and are supplied by C.D.H, Thomas Baker, Himedia, and Merck (Sigma Aldrich) companies without any additional purification processes (ethanol absolute, glacial acetic acid, P-aminophenol, Salicylaldehyde, sodium nitrite, hydrochloric acid, sodium hydroxide, 2-Aminothiazole, and Nickel (II) chloride hexahydrate).

2.2- Instrumentation:

All techniques that were used in the characteristic study of the new synthesized ligand and its complexes were a UV-Vis spectrophotometer (Jenway 7315, England), FT-IR spectrophotometer (Shimadzu IRPrestige 21, Japan), pH-meter (inolab WTW 530, Germany), Digital Conductivity meter (inolab WTW 7310, Germany), Melting point instrument SMP 30 (Stuart, England), Balance BL 2105 (Sartorius, Germany), ^{1}H-NMR Spectrophotometer (Bruker 400 MHZ, Germany).

2.3- Experiments:

2.3.1- Preparation of the Ligand

In the first step (Schiff), a solution of p-aminophenol (0.02mole, 2.1826g) dissolved in absolute ethanol (5mL) was mixed with a solution of salicylaldehyde (0.02mol, 2.4424 g) dissolved in absolute ethanol (5mL), then three drops of glacial acetic acid were added to the mixture as a catalyst, the reaction mixture was refluxed for (3–4) hours at (70–80C°), and the reaction progress was monitored using Thin Layer Chromatography (TLC), Upon completion, the mixture was cooled to room temperature and subsequently placed in an ice bath for 30 minutes, the resulting yellow crystalline precipitate was filtered, air-dried, and recrystallized from absolute ethanol, the product was then washed with hexane to remove unreacted starting materials and dried in an oven at 45C° for 30 minutes, finally the solid product was ground, weighed, and stored in an amber bottle, with a final yield of (95.08%)[11].

In the second step (Azo), 2-aminothiazole (0.02mole, 2.0028g) was dissolved in a mixture of 10 mL HCl (2 M) and 20 mL distilled water, the resulting solution was cooled in an ice bath at (0–5)C° for 10 min, a solution of sodium nitrite (0.022mole, 1.518g) in 7.5 mL distilled water was then added dropwise with continuous stirring and cooling over 30 min to effect diazotization, After completion, urea (0.001mole, 0.0606g) was introduced to quench excess nitrous acid, and the mixture was maintained for an additional 10 min, the diazonium solution was added gradually to a pre-cooled Schiff base solution that had been prepared 30 min earlier by dissolving the Schiff base (0.01 mole, 2.1324 g) in 10 mL absolute ethanol and sodium hydroxide (0.025 mole, 1g) in 10 mL distilled water, under continuous stirring at (0-5)C°, the reaction mixture developed a dark-brown color at pH 9.5 and was stirred for 15 min to complete formation of the Schiff–azo ligand, the pH was then adjusted to (7.15) with dilute hydrochloric acid, precipitating a reddish-brown solid, the suspension was allowed to stand for 15 min to ensure complete precipitation, then the solid was collected by filtration and

washed repeatedly with cold distilled water, the crude product was air-dried, recrystallized from absolute ethanol, and oven-dried at 45 C° for 30 min. The dried material was ground, weighed, and stored in a dark container. The yield was 75.27%, and its melting point was measured and found to be approximately (121-123)C° As illustrated in Scheme 1 [12].

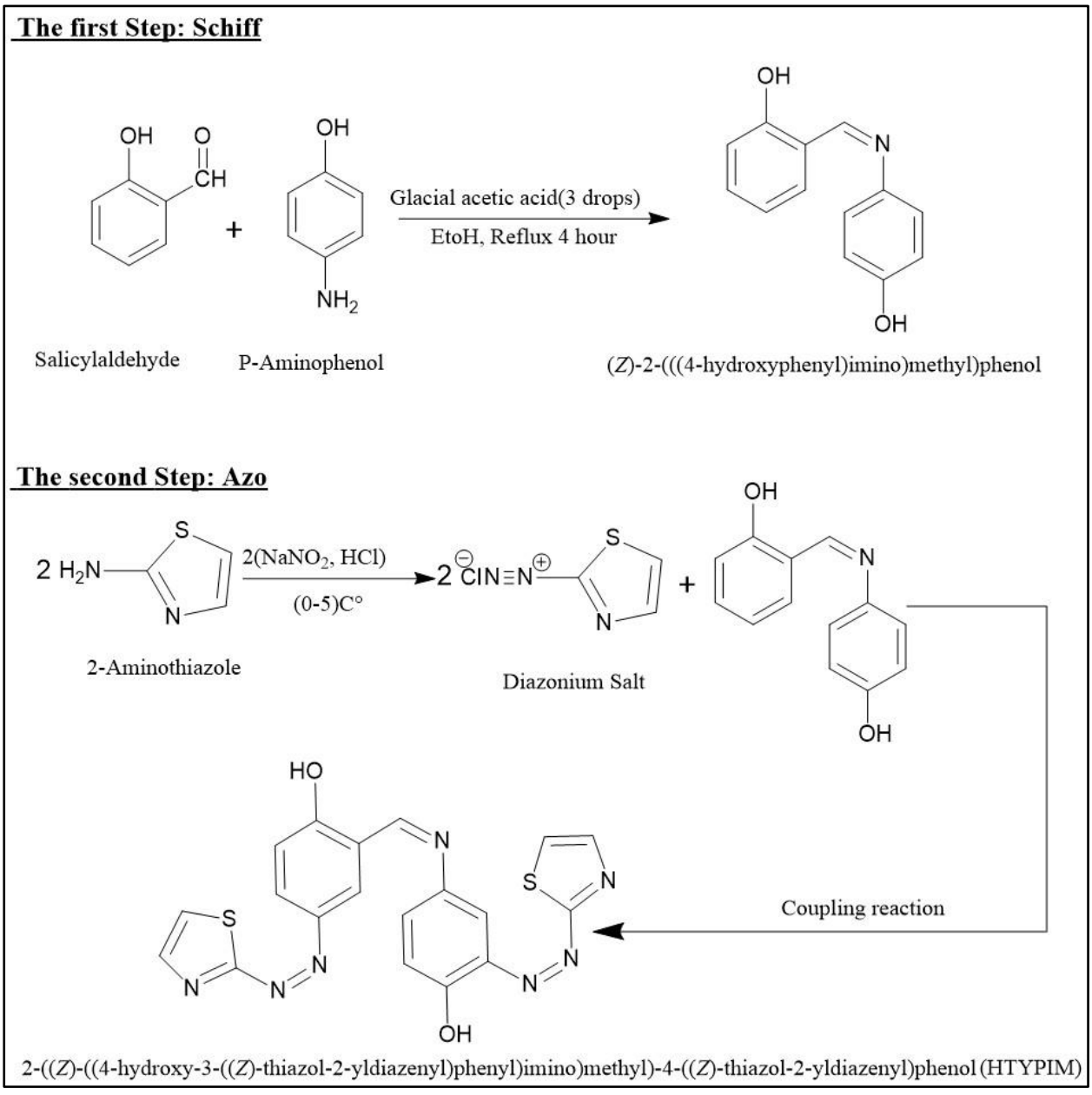

Scheme 1. The steps to preparation of ligand

2.3.2- Preparation of Standard Solutions:

A ligand solution with a concentration of (1×10^{-4}M) was prepared by dissolving (0.0043g) of the ligand in absolute ethanol and was placed in a (100mL) volumetric

flask, the nickel (II) ion solution was prepared at a concentration of (1×10^{-4}M) by dissolving (0.0023g) of nickel (II) chloride hexahydrate in deionized water and was placed in a (100mL) volumetric flask, the buffer solution was prepared at a concentration of (0.01M) by dissolving (0.7708g) of ammonium acetate in deionized water and was placed in a (1000mL) volumetric flask, from this solution several (100mL) volumetric flasks were prepared covering the pH range (4–11) by adding drops of diluted ammonium hydroxide or diluted acetic acid.

3. Results and Discussion:

3.1- Study of ultraviolet –visible spectra for ligand and Ni (II)complex

Ligand and nickel complex solutions were prepared at a concentration of (1×10^{-5}M) and placed in two 10 mL volumetric flasks and using absolute ethanol as the Blank solution, a spectroscopic survey of the ligand and the nickel complex was conducted in the ultraviolet-visible region of the spectrum and within the range (200-700)nm, in the electronic spectrum of the ligand showed three bands at (λ= 233) nm, (λ= 272) nm and (λ= 350) nm, while in the Ni (II) complex spectrum showed three absorption bands at (λ= 296) nm, (λ= 342) nm identified for charge transition (C.T.) and (λ_{max}= 417) nm, as show in (Figure 1, 2) [13].

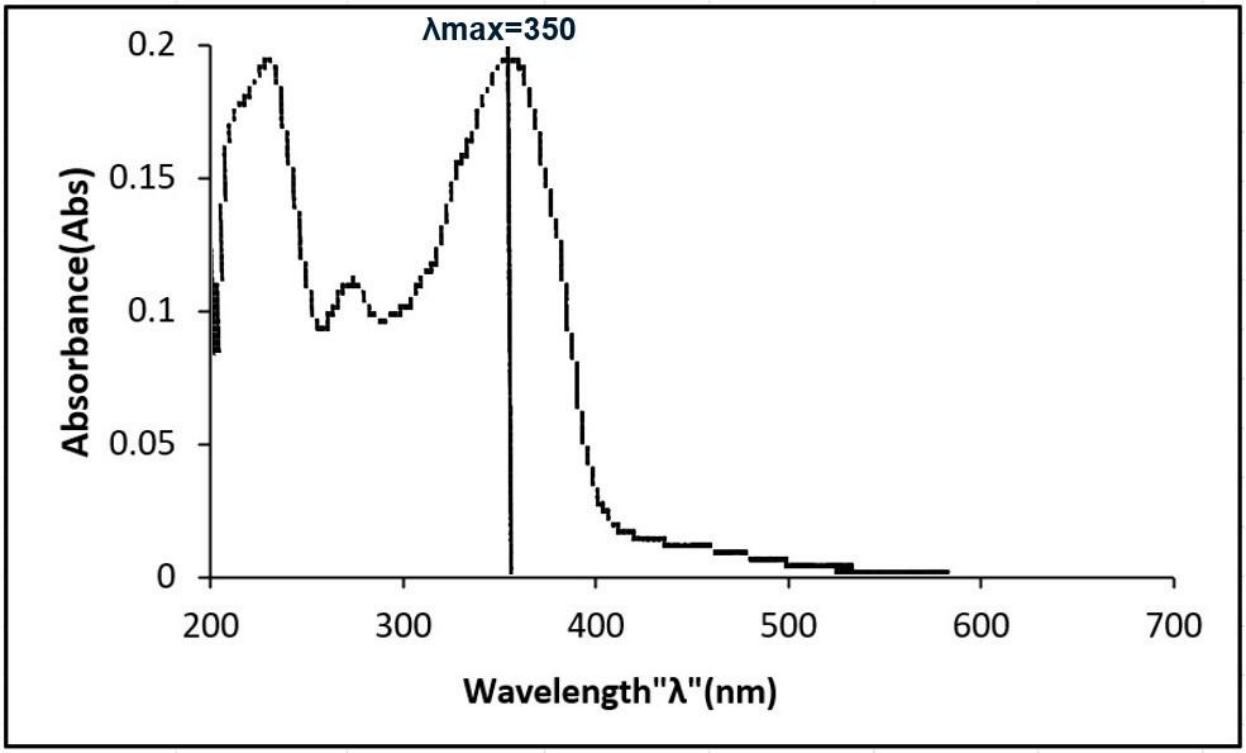

Figure 1. Ultraviolet-visible spectrum of Ligand.

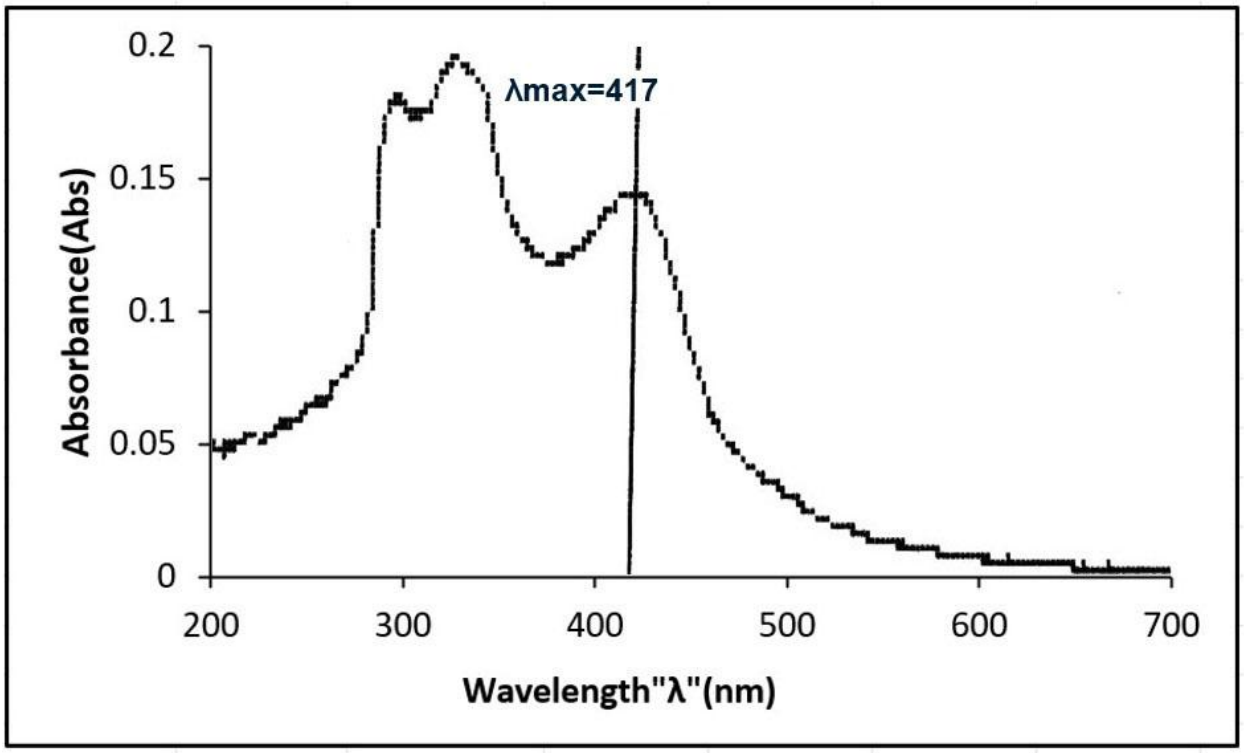

Figure 2. Ultraviolet-visible spectrum of Ni (II) complex.

3.2- Study FT-IR spectra for ligand and Ni (II) complex

The FT-IR spectrum of the prepared new ligand and Ni (II) complex respectively shows a broad band belonging to (νO-H) at (3410, 3387)cm^{-1} due to hydrogen bonding, a band at (1618, 1616)cm^{-1} belonging to (νC=N), a band at (1508, 1506) cm^{-1} belonging to (νN=N), a band at (1280, 1280) cm^{-1} belonging to (νC-O), a band at 563 cm^{-1} belonging to (νM-O), a band at 497 cm^{-1} belonging to (νM-N), the band values reveal a shift toward lower frequency and the appearance of new bands, absent in the ligand spectrum, indicating the occurrence of coordination, as show in (Figure 3, 4) [14].

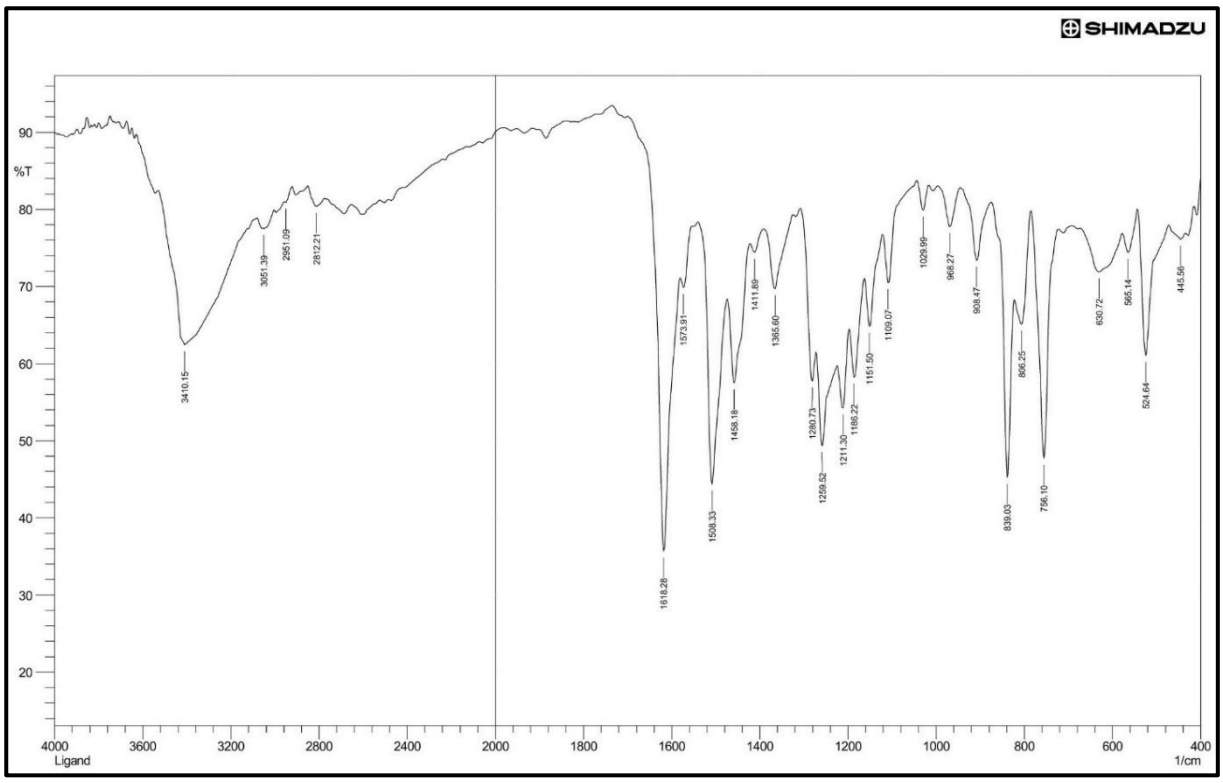

Figure 3. FT-IR spectrum of ligand.

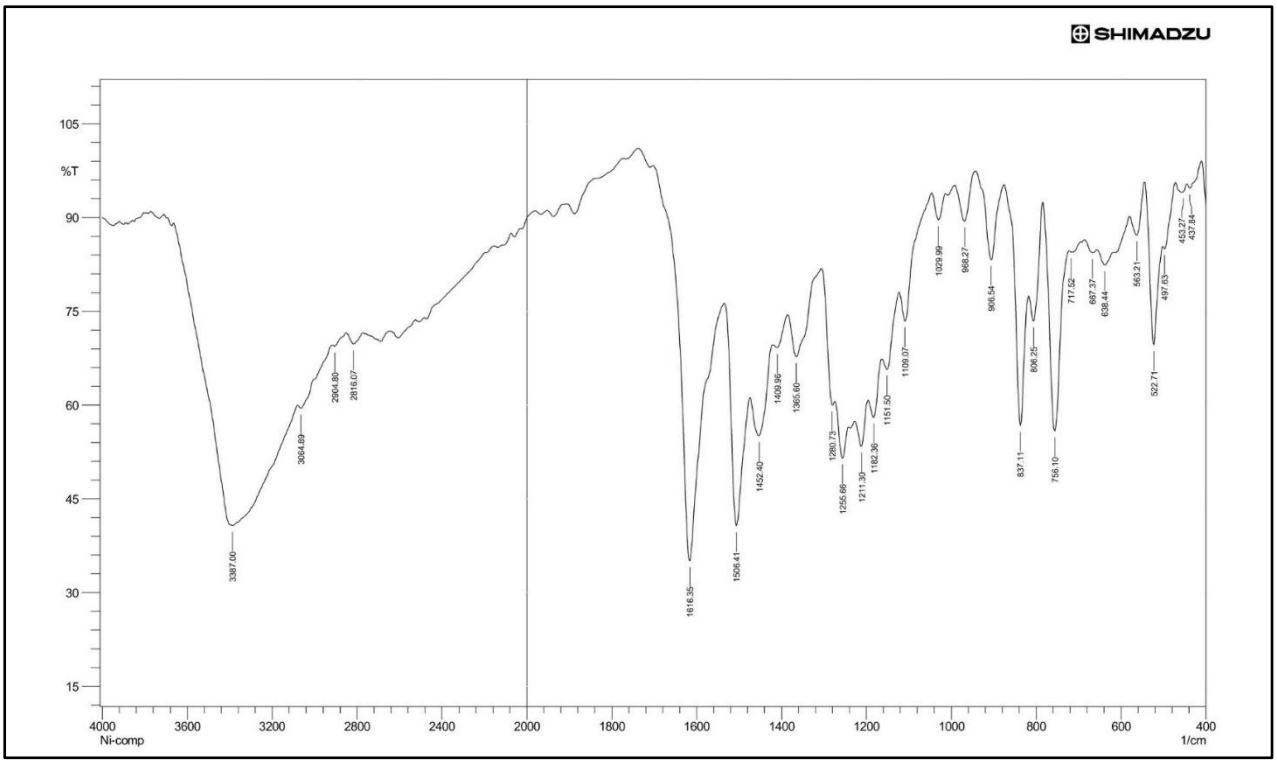

Figure 4. FT-IR spectrum of Ni (II) complex.

3.3- [1]HNMR spectrum for ligand and Ni (II) complex

From the signals appearing in the spectrum 1HNMR for ligand and Ni (II) complex respectively, the singlet signal at (δ=13.42,13.37ppm,1H) refers to the proton of the Phenolic (OH) group adjacent to the azomethine group (CH=N), Another singlet signal was observed, corresponding to the proton of the second phenolic OH group adjacent to the azo (N=N) at (9.67, 9.70ppm,1H) the reason for its appearance at a position very close to that in the free ligand indicates that this group is relatively distant from the coordination center of the nickel complex, while the singlet signal of the azomethine proton (CH=N) appears at (8.90,8.86ppm,1H) this signal is highly characteristic of Schiff bases and its presence provides strong evidence for the formation of the bond and the chemical shift of the signal confirms the occurrence of coordination, whereas multiple signals appeared within the range of (6.83–7.61ppm) and (6.80-7.58), corresponding to the protons of the aromatic rings (benzene and thiazole), with a total of (10H), the signal at (3.34,3.32ppm) indicates the presence of moisture H_2O and the signal at (2.50-2.52 ppm) and (2.50ppm) indicates the solvent DMSO-d^6, as illustrated in (Figure 5, 6) [15].

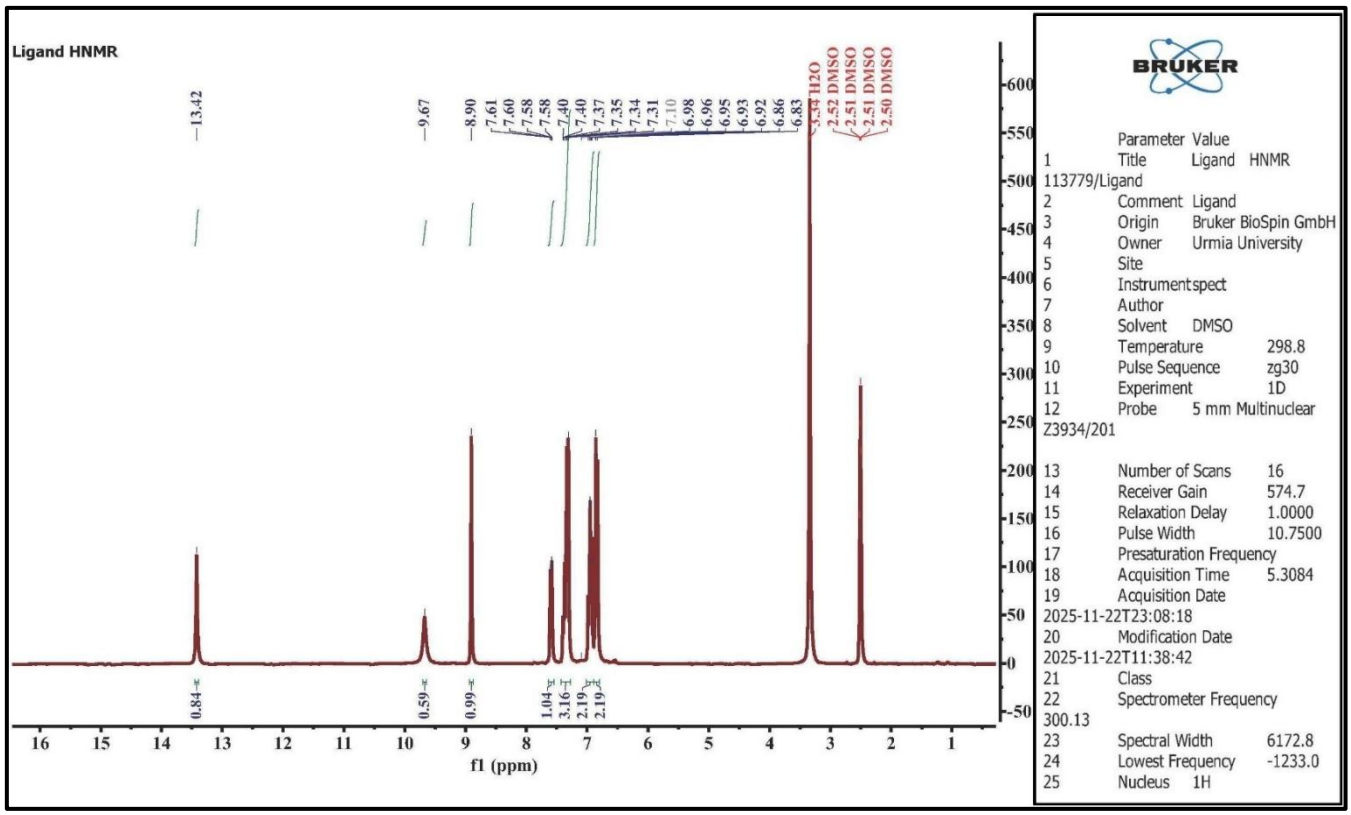

Figure 5. [1]HNMR spectrum for ligand.

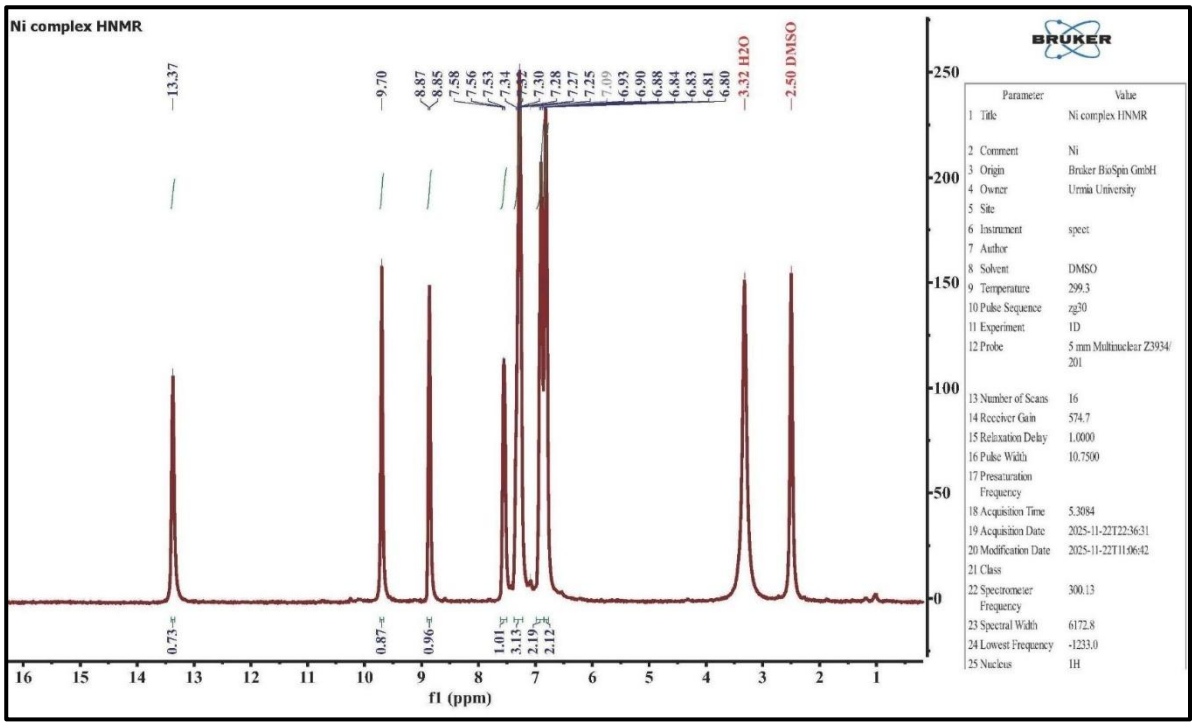

Figure 6. [1]HNMR spectrum for Ni (II) complex.

3.5- Study the optimum condition for the nickel (II) complex

3.5.1- pH effect

A wide range of buffer solutions were chosen, ranging from pH (4-11) by measuring the absorption at the maximum wavelength of the nickel complex and at the concentration ($1x10^{-5}$M), in (Figure 7) it was shown that the absorption increased at pH = 8 [16].

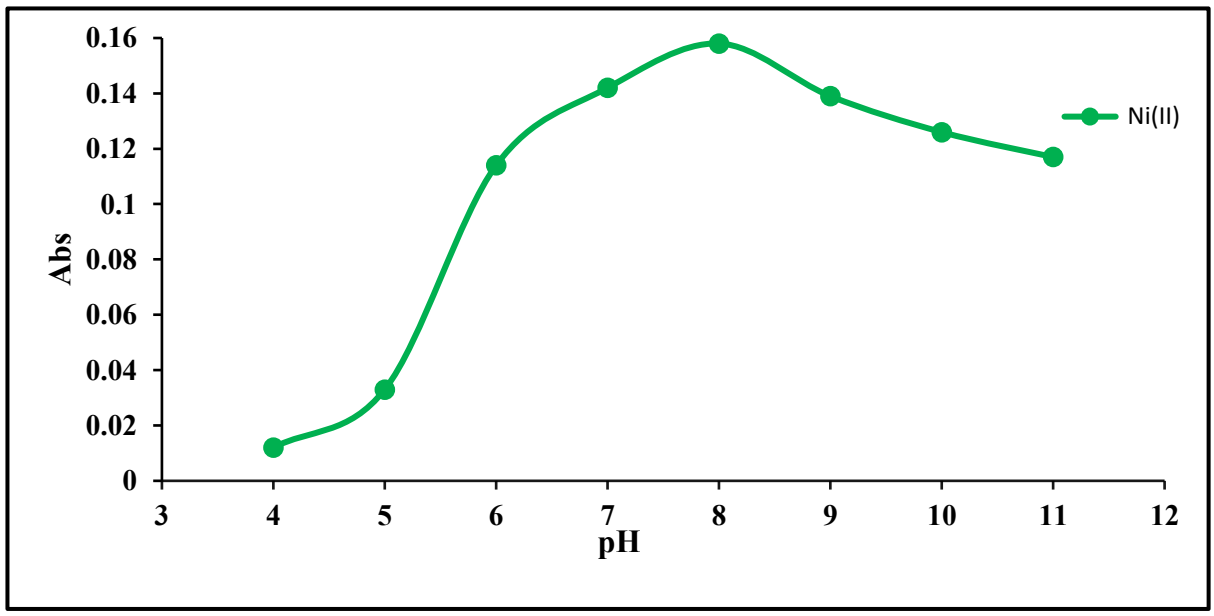

Figure 7. Effect of pH value in Ni (II) complex.

3.5.2- Effect of ligand concentration

A set of volumetric flasks (10 mL capacity) was prepared, each containing (1mL) of nickel ion solution at a concentration of (1×10^{-4}M) was added then different volumes of the ligand solution with a concentration (0.5×10^{-4}-5×10^{-4}M), and the volume was completed with the buffer solution at pH=8 to obtain a wide range of concentrations (0.5×10-$5^{-5}\times10^{-5}$M), then The absorbance of all solutions was measured at (λ_{max}= 417nm) against the reagent and ethanol as blank solution, where it was found that the best concentration of the ligand It is (4×10^{-5}M), as illustrated in (Figure 8) [17].

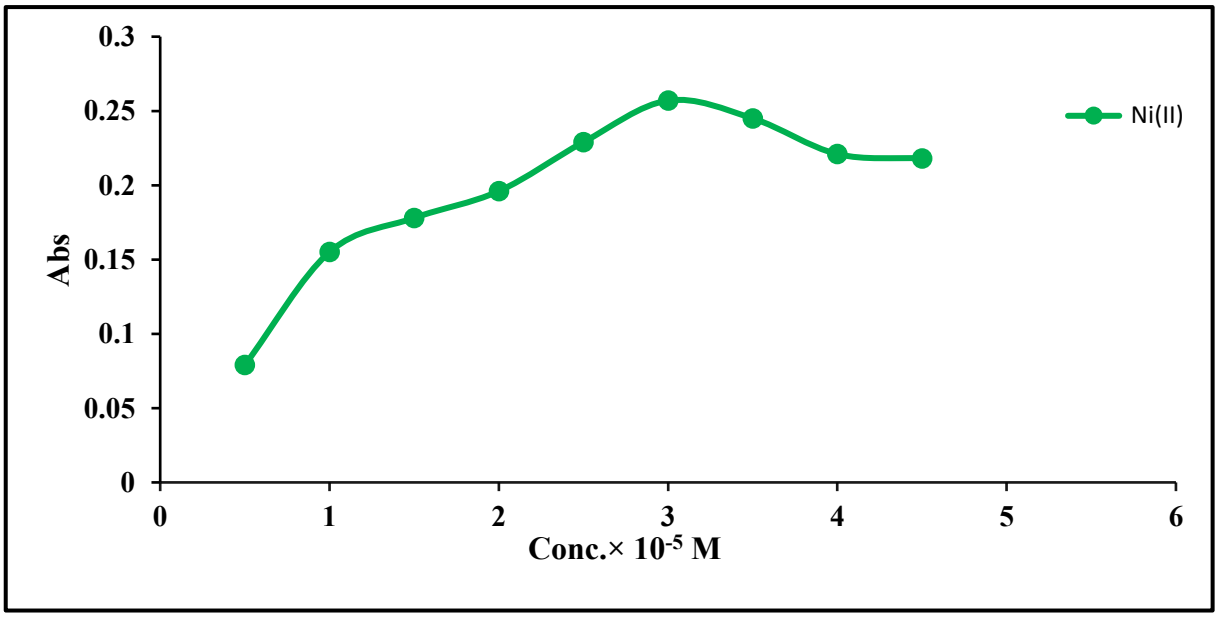

Figure 8. Effect of ligand concentration on Ni (II) complex.

3.5.3- Effect time on stability of nickel (II) complex

A set of volumetric flasks (10 mL capacity) was prepared, each containing (1mL) of nickel ion solution at a concentration of (1×10^{-4}M), Subsequently (1mL) of the optimal ligand concentration (4×10^{-4}M) was added to each flask, and the volume was completed with the optimal buffer solution at pH 8, The absorbance of all solutions was measured at (λ_{max}=417nm) against the reagent and ethanol as blank solution, at different time intervals ranging from (10-90) min, It is observed from the (figure 9) that the absorbance remains constant, which demonstrates that the prepared nickel complex exhibits high stability and persistence [18].

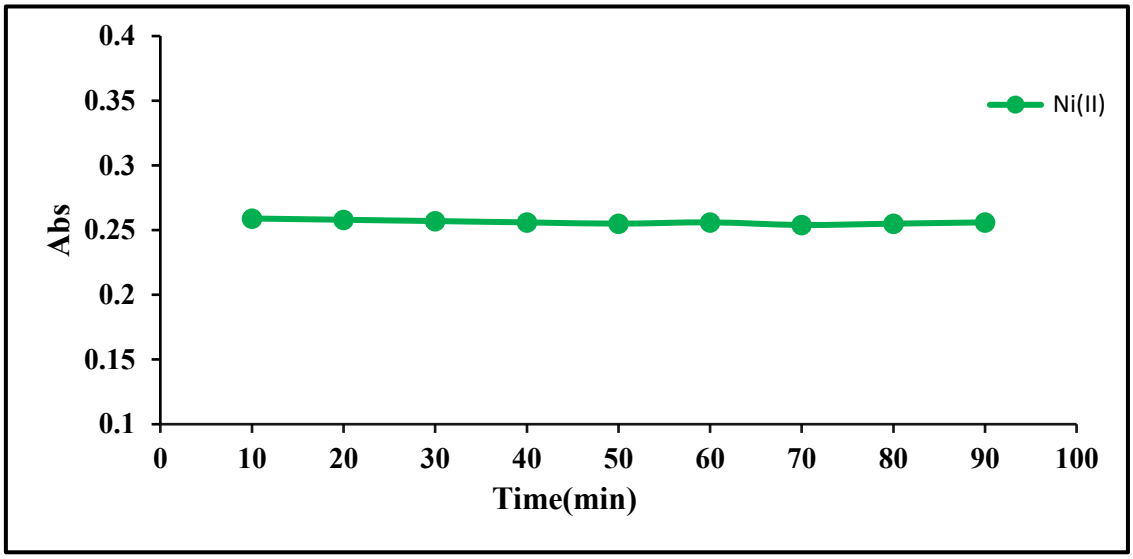

Figure 9. Effect time on stability of Ni (II) complex.

3.5.4- Effect of temperature in stability of nickel (II) complex

A set of volumetric flasks (10 mL capacity) was prepared, each containing (1mL) of nickel ion solution at a concentration of (1×10^{-4}M), Subsequently (1mL) of the optimal ligand concentration (4×10^{-4}M) was added to each flask, and the volume was completed with the optimal buffer solution at pH=8, The solutions were placed in a water bath with a temperature range of (10–70C°), The absorbance of all solutions was measured at (λ_{max}=417nm) against the reagent and ethanol as blank solution, the absorbance values of the complex reach their peak and give the best color intensity at the temperature between (10-25C°) and then the absorbance of the complex decreases with increasing temperature, This is due to dissociation of the complex at high temperatures, As shown in (Figure 10) [19].

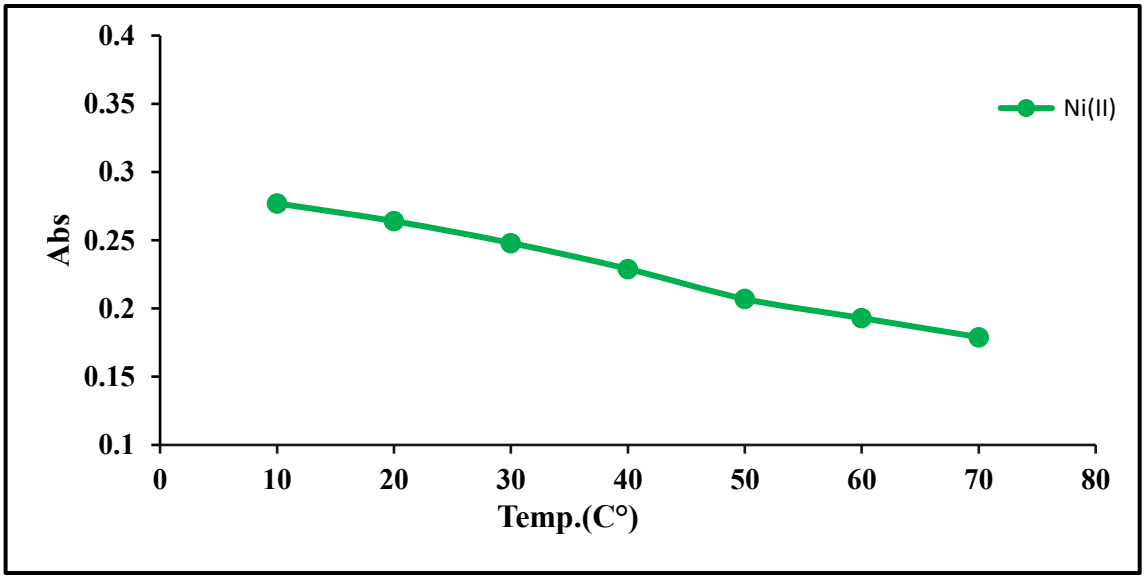

Figure 10. Effect of temperature in stability of Ni (II) complex.

3.5.5- Study the effect of the order of addition for the nickel complex

The complex solution was prepared in the same manner as in the above studies, but with a different order of addition. The purpose of this study is to determine the best addition order to form the nickel complex under optimal conditions. The first case, as shown in Table 1, was chosen as the best addition because it gives the highest absorption [20].

Table 1. Effect of the Ni (II) complex composition's order of addition

Sequence of addition number	Sequence of addition	Abs. of Ni (II) complex
1	M+R+pH	**0.255**
2	R+M+pH	0.248
3	M+pH+R	0.242
4	pH+M+R	0.239

Where: M = Ni (II), R = Reagent, pH = Buffer solution.

3.6- Study of explanation of the calibration curve for nickel complex

A set of volumetric flasks (10 mL capacity) was prepared, each containing 1 mL of the Ni (II) solution at different concentrations ranging from (1×10^{-7}-1×10^{-4}M) this corresponds to (0.0058-5.869µg·L^{-1}) of nickel ion, Subsequently, 1 mL of the optimal concentration of reagent (3×10^{-4}M) was added to each flask, and the volume was completed with the optimal buffer solution for Ni (II) complex at pH=8, the absorbance of all solutions was then measured at λ_{max}=417 nm against the reagent and ethanol as blank solution, the concentrations that obey the Beer-Lambert law were determined for the copper complex by drawing a calibration curve, many concentrations were excluded due to their deviation from the Beer- Lambert law and the appearance of absorption peaks outside the measurement limits, therefore the concentrations that obey the Beer-Lambert law are (0.05-1.25)µg.L^{-1}, as shown in (Figure 11), and (Table 2) shows some characteristics of the calibration curve for the copper which was extracted using this equations [21]:

$$A = \varepsilon bc \qquad \text{Eqn. 1}$$

$$S = \frac{At.wt}{\varepsilon} \qquad \text{Eqn. 2}$$

$$L.O.D = \frac{3 \times S.D.}{SLOP} \qquad \text{Eqn. 3}$$

$$L.O.Q = \frac{10 \times S.D}{SLOP} \qquad \text{Eqn. 4}$$

Where ε = Molar absorptivity, A= Absorbance, b= Path length cell (1cm), C= Molar concentration, S = Sandell's sensitivity, At.wt = Atomic weight, L.O.D = limit of detection, L.O.Q = limit of quantification

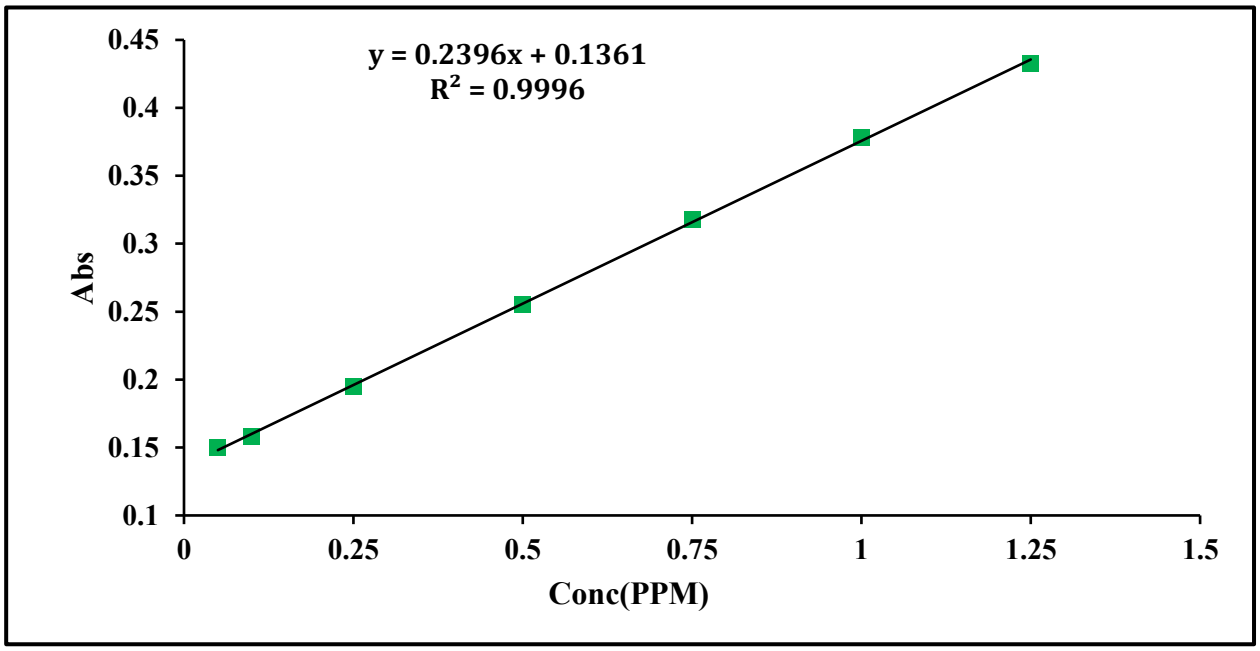

Figure 11. Calibration curve for Ni (II) complex.

Table 2. Some properties of the calibration curve for Cu (II) complex.

Conc. obey the Beer-Lambert law (µg/mL)	Straight-line equation	slope	ε (L/mol.cm)	S (µg.cm^{-2})	R^2	L.O.D (µg/mL)	L.O.Q (µg/mL)
(0.05-1.25)	y=0.2396x+ 0.1361	0.2396	1.764×10^5	3.327×10^{-4}	0.9996	0.0075	0.025

3.7- Study the stoichiometry composition of nickel complex

Two methods were used to appoint the ratio of metal to ligand, the molar ratio method and the continuous variation method:

In molar ratio method, a set of 10 mL volumetric bottles, several solutions were prepared containing a fixed concentration of nickel ion solution with a variable concentration of ligand solution, and complete the volume with the best pH=8 value, and then the absorbance was measured at the maximum wavelength, the results of the study showed that the ratio [metal:ligand] is [1:2], in continuous variation method different volumes of the nickel ion solution (0.5-4) ml were mixed with different volumes of the ligand (4-0.5) ml solution, and the results gave that the ratio between [metal:ligand] is [1:2], as shown in (Figure 12, 13) [22].

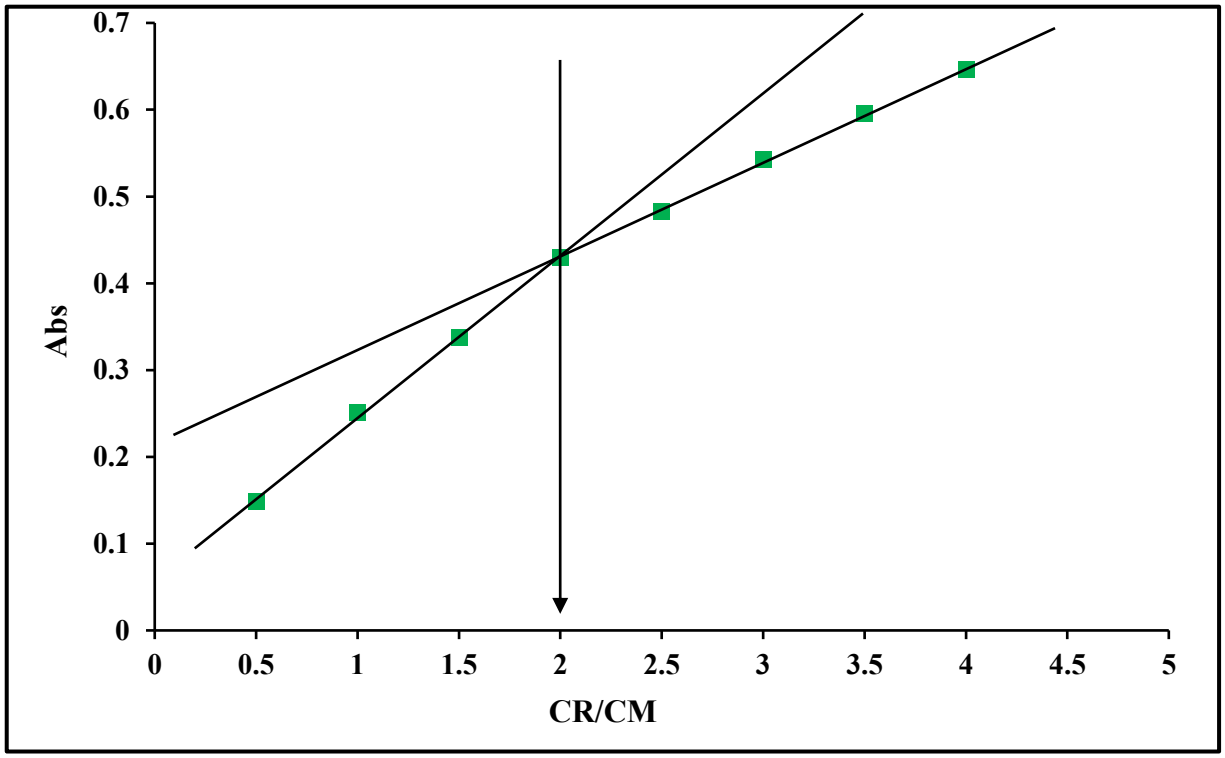

Figure 12. Stoichiometry composition of the molar ratio method of Ni (II) complex.

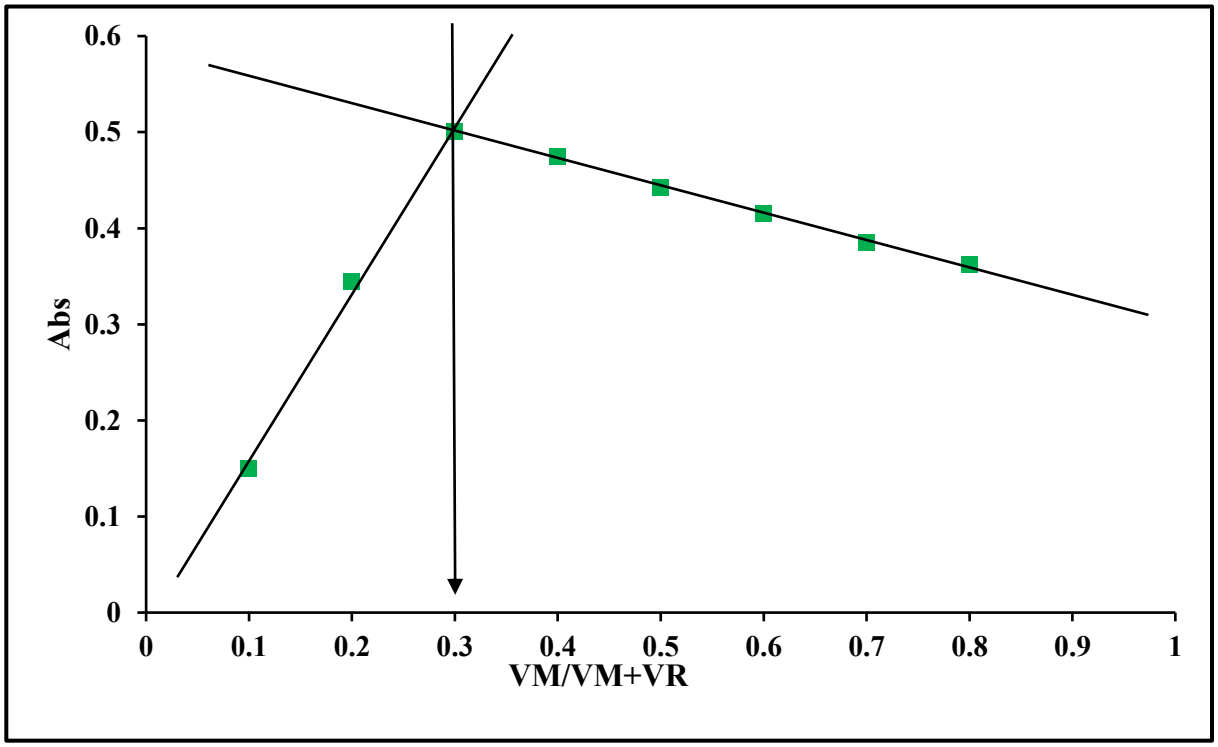

Figure 13. Stoichiometry composition of continuous variation method of Ni (II) complex.

3.7.1- Calculation of the stabilization constant for complex

The stability of the nickel complex with the ligand was studied by calculating the degree of dissociation and the stability constant based on the absorption values obtained As shown in the (Table 3), From the results, it is clear that the complex have a high degree of stability, which enhances the possibility of using the detector in the spectral estimation of these elements, Which was extracted using the following equations [23]:

$$M^{+2} + 2L \leftrightharpoons ML_2 \qquad \text{Eqn. 5}$$

$$\alpha c \quad 2\alpha c \quad (1-\alpha)c \qquad \text{Eqn. 6}$$

$$K_{st} = \frac{(1-\alpha)c}{(\alpha c)(2\alpha c)^2} \qquad \text{Eqn. 7}$$

$$K_{st} = \frac{(1-\alpha)}{4(\alpha^3 c^2)} \qquad \text{Eqn. 8}$$

$$K_{inst} = \frac{1}{kst.} \qquad \text{Eqn. 9}$$

$$\alpha = \frac{Am - AS}{Am} \qquad \text{Eqn. 10}$$

Where M = Nickel ion, L = Ligand, α= Degree of Dissociation, C = Molar concentration of the complex, $K_{st.}$ = Stability constant, $k_{inst.}$= Instability constant, Am = The absorption of the complex is at its maximum value, As = Absorption of the complex at the equivalence point.

Table 3 shows the absorption values (Am) and (As) of the nickel complex, as well as the values of (α), (Kst.), and ($K_{inst.}$)

The controlling metal ion	As Value	Am Value	α	K_{st} mol.L^{-1}	K_{inst} L.mol^{-1}	Log K_{st}
Ni (II)	0.430	0.646	0.3343	4.4546×10^{8}	2.2448×10^{-9}	8.6488

3.7.2- Studying the effect of thermodynamic functions (ΔG⁰, ΔH⁰, ΔS⁰) on the formation of the copper complex

This study aims to know the effect of temperature on the thermodynamic functions of the nickel complex, which were calculated as shown in Table 4 and Figure 14. It is clear from the results in (Figure 14) for the nickel complex that a negative enthalpy value (ΔH^0) indicates that the reaction is exothermic, and this is due to the strong bonding between the metal ion and the ligand to form the complex, and that negative (ΔG^0) values indicate the Spontaneity interaction of the reaction, As it is known, a positive value of entropy(ΔS^0) is a measure of randomness, so a negative value of entropy indicates a decrease in randomness and was extracted using this equations [24]:

$$\Delta G^\circ = -2.303\, R\, T\, log Kst \qquad \textbf{Eqn. 11}$$

$$Slope = \frac{-\Delta H^\circ}{2.303R} \qquad \textbf{Eqn. 12}$$

$$\Delta G^\circ = \Delta H^\circ - T\Delta S^\circ \qquad \textbf{Eqn. 13}$$

Where ΔG= The change in Gibbs free energy, R = gas constant (8.314 $J.mol^{-1}.k^{-1}$), ΔH = the change in enthalpy, ΔS = the change in entropy, and T = temperature in kelvin.

Metal ion complex	T(K)	$1/T\times10^3$ (k^{-1})	Log K_{st}	-ΔG° (KJ/mole)	-ΔH° (KJ/mole)	ΔS° (KJ/mole.k)
Ni(II)	288	3.47	8.7652	48.3346	0.00458	0.1678
	298	3.35	8.5438	48.7496		0.1635
	308	3.24	8.3304	49.1270		0.1594
	318	3.14	8.1556	49.6577		0.1561
	328	3.04	7.9823	50.1309		0.1528
	338	2.95	7.8047	50.5099		0.1494

Table 4: Temperature's effect on thermodynamic performance for Ni(II) complex.

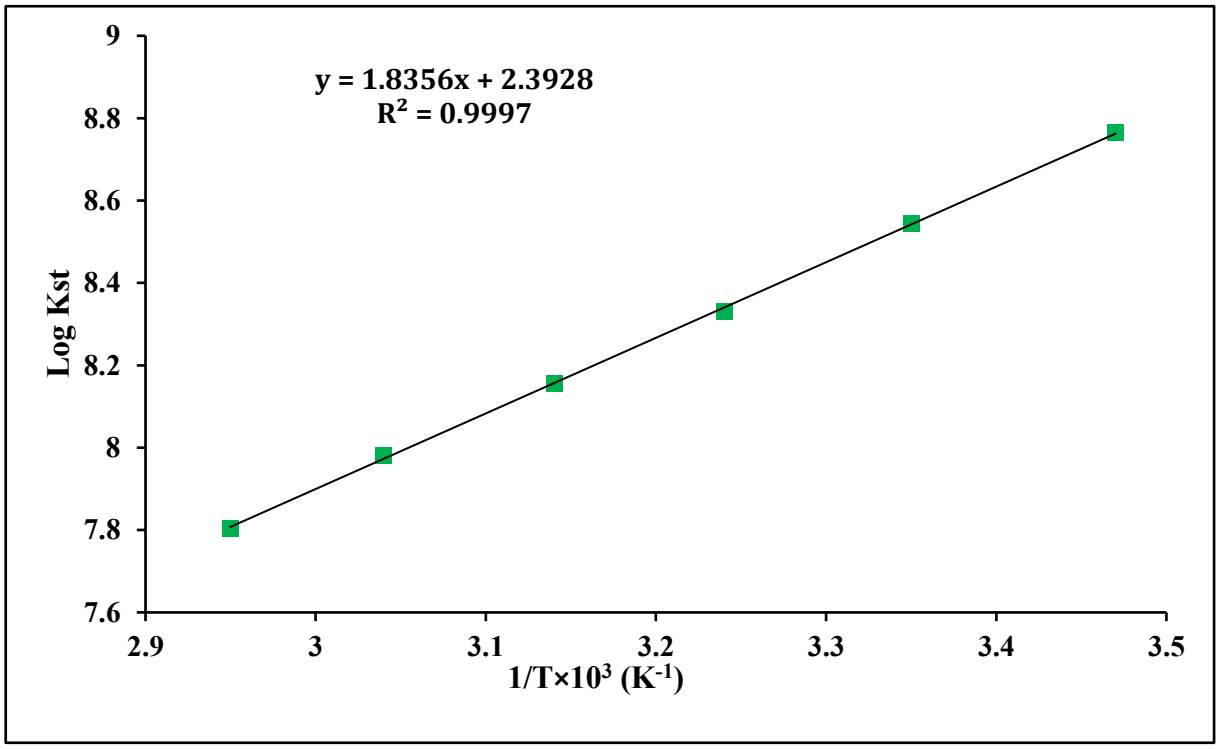

Figure 14. The relationship between (Log Kst) and (1/T) for the Ni (II) complex.

3.8- Statistical processing of results

3.8.1- Precision

done Calculation the values of the standard deviation (S.D) and the relative standard deviation (RSD%) for the nickel complex under ideal conditions to ensure the accuracy of the analytical method by using the following equations, and they are displayed in (Table 5) [25]:

$$X' = \sqrt{\frac{\sum xi}{N}} \qquad \textbf{Eqn. 13}$$

$$S.D = \sqrt{\frac{\sum(xi-x')^2}{N-1}} \qquad \textbf{Eqn. 14}$$

$$RSD\% = \frac{S.D}{X} \times 100\% \qquad \textbf{Eqn. 15}$$

Where: xi = Reading for every absorption, x' = mean, N = Number of readings

Table 5. Values for standard deviation and relative standard deviation for the Ni (II) complex

Metal ion complex	Conc. of ion(ppm)	S.D	R.S.D%
Ni(II)	0.05	0.0006	0.3937
	0.5	0.0011	0.4290
	1.25	0.0015	0.3472

3.8.2- Accuracy

The accuracy of the analytical method for the copper complex was determined by calculating the absolute error (d), relative error (Er%), and recovery percentage (Re%) for the nickel complex using the absorbance readings of the calibration curve under ideal conditions. The method proved to be sensitive and accurate, and these results are displayed in Table 6 [26]:

$$d = Experimental\ value - True\ value \qquad \textbf{Eqn. 16}$$

$$E_{rel}\% = \frac{d}{\mu} \times 100\% \qquad \textbf{Eqn. 17}$$

$$Re\% = 100 \pm E_{rel}\% \qquad \textbf{Eqn. 18}$$

Table 6. Relative error (d), absolute error (Erel%), and recovery percentage (Re%)

Complex of metal ion	Analytical value(ppm)	d	Erel%	Re%
Ni (II)	0.05	-0.0024	-1.57	98.43
	0.5	-0.0014	-0.54	99.46
	1.25	0.001	0.23	100.24

values for the nickel complex.

3.9- Preparation of solid nickel complex

The complex was prepared in a molar ratio [metal: ligand] [1:2] by adding (0.002mol, 0.8709g) of ligand dissolved in 20mL of absolute ethanol to (0.001mol, 0.2376g) of nickel chloride hexahydrate ($NiCl_2.6H2O$) dissolved in 10mL of the best buffer solution (pH= 8), with the best conditions for the complex fixed, was heated to a temperature of (70-80)C° for an (1-2)hour, then left aside to precipitate, it was observed that a precipitate with a blackish-green color formed and it was recrystallized with absolute ethanol, and the yield percentage was (69.24%), the melting point was measured to be approximately (133-135)C° [27].

3.10- Molar electrical conductivity of the nickel complex

The molar electrical conductivity of a solution of solid copper complex at a concentration of (1×10^{-3}M) was measured in pure (DMSO) solvent and at laboratory temperature, It was shown from the conductivity result in Table 7 that the nickel complex it is an electrolyte with neutral charge, it contains two chloride ions outside the coordination sphere to balance the charge, in a [1:2] ratio [28].

Table 7. Conductivity values for the Ni (II) complex in (DMSO).

Molecular formula	Molar electrical conductivity ($Ohm^{-1}.mole^{-1}.cm^2$)
$[Ni(C_{19}H_{13}O_2N_7S_2)_2(H_2O)_2]Cl_2$	136

3.11- The solubility of solid nickel complex

The solubility of the ligand and nickel complex was studied in a number of solvents and the results are shown in the Table 8 [29].

Table 8. Solubility of ligand and copper complex in different solvents

Solvent	Ligand	Complex of Ni (II)
Water	-	-
Methanol	÷	÷
Ethanol	+	+
Acetone	+	+
DMSO	+	+
DMF	+	+
Chloroform	÷	÷

Where: (+) = Complete dissolution, (-) = Undissolved, (÷) = Partial dissolution

3.12- The Magnetic susceptibility of the nickel complex

The magnetic susceptibility of the prepared solid nickel complex was measured at laboratory temperature (17C°) using the Faraday method to obtain the gram susceptibility values (X_g). Based on Pascal's constants, the effective magnetic moment (μeff) was calculated and compared with the theoretical magnetic moment according to the following equations [30]:

Theoretical magnetic moment equation:

$$\mu_S = \sqrt{n(n+2)}$$

Equations of the practical effective magnetic moment:

$$X_M = X_g \times M.wt$$

$$X_A = X_M - D$$

$$D = (-M.wt_{comp.}/2) \times 10^{-6}$$

$$\mu_{eff} = 2.828\sqrt{X_A.T}\ B.M$$

Where: n= number of unpaired electrons of the central atom, T= absolute temperature X_M= molar susceptibility X_A= atomic susceptibility, X_g= Gravimetric susceptibility D= Magnetic correction factor, B.M.= Bohr Magneton, μ_{eff}= Effective magnetic moment $M.wt_{Comp.}$=

Magnetic susceptibility results revealed that the nickel, copper, and cobalt complexes exhibit paramagnetic characteristics and possess octahedral geometries, as illustrated in Table Table 9.

Table 9. presents the magnetic susceptibility measurement of the Ni (II) complex

Metal complex	Ni (II)complex
Xg	0.041×10^{-4}
X_M	0.004545465
D	-0.000554325
X_A	0.005099790
μ_{eff}	3.4391
T(K)	17+273=290

3.13- The proposed geometrical structure of nickel complex

Based on the literature concerning the available coordination sites of the ligand and its binding mode with the nickel ion, and in light of the obtained results it can be concluded that the ligand behaves as a bidentate, it coordinates with the metal ion at a ligand-to-metal molar ratio [L:M] of [1:2] for the copper complex, accordingly the proposed geometric structure of the nickel complex is octahedral with (sp^3d^2) hybridization, as illustrated in Scheme 2 below [31]:

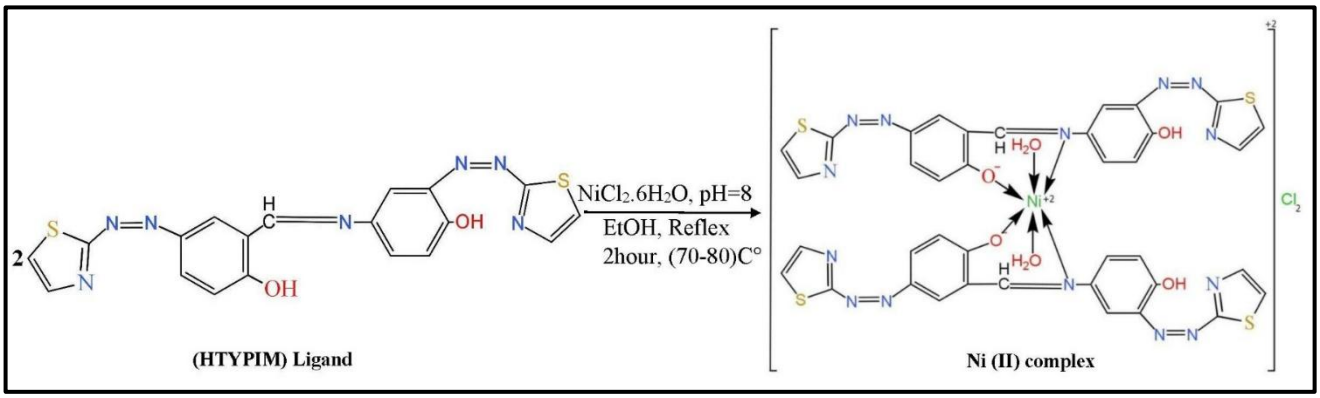

Scheme 2. The proposed geometric structure of Cu (II) complex.

3.14- Conclusion

A new organic Schiff-Azo ligand was prepared from simple, available and cheap materials in two steps. The first step includes preparation of a Schiff base from the condensation reaction of salicylaldehyde with p-aminophenol, and the second step includes diazotization reaction of a Schiff base with 2-aminothiazole for the synthesis of the ligand, the prepared ligand and complex were characterized by Ultraviolet-Visible, FT-IR, ^{1}HNMR spectra, It was used as a ligand to determine small amounts of nickel (II) ion by the reaction of the ligand with the copper ion to form a highly stable colored complex at pH=8 and the metal to ligand ratio was [1:2], this method proved, through the results obtained, It exhibits high sensitivity and selectivity for nickel ion determination, based on the measurements the geometry of the nickel complex is octahedral.

References

[1] Greenwood, N. N., & Earnshaw, A. (2012). *Chemistry of the elements* (2nd ed.). Elsevier.

[2] Housecroft, C. E., & Sharpe, A. G. (2018). *Inorganic chemistry* (5th ed.). Pearson.

[3] Anthony, J. W., Bideaux, R. A., Bladh, K. W., & Nichols, M. C. (2003). *Handbook of mineralogy: Nickel minerals*. Mineral Data Publishing.

[4] Crundwell, F. K. (2013). *Extractive metallurgy of nickel, cobalt, and platinum-group metals*. Elsevier.

[5] Lide, D. R. (2004). *CRC handbook of chemistry and physics* (85th ed.). CRC Press.

[6] Buschow, K. H. J. (2003). *Handbook of magnetic materials*. Elsevier.

[7] Greenwood, N. N., & Earnshaw, A. (2012). *Chemistry of the elements* (2nd ed.). Elsevier.

[8] Hamid, S. S. (2025). Spectroscopic insights into ligand field effects on nickel(II) complexes. *International Journal of Advanced Chemistry Research, 7*(2), 13–21. https://doi.org/10.33545/26646781.2025.v7.i4a.271

[9] Zhang, W., & Zhang, Y. (2020). Nickel-based materials for rechargeable batteries. *Journal of Power Sources, 450*, 227636. https://doi.org/10.1016/j.jpowsour.2019.227636

[10] Yusuf, T. L., Oladipo, S. D., Zamisa, S., Kumalo, H. M., Lawal, I. A., Lawal, M. M., & Mabuba, N. (2021). Design of new Schiff-base copper(II) and nickel(II) complexes: Synthesis, crystal structures, DFT study, and binding potency. *ACS Omega, 6*(19), 13704–13718. https://doi.org/10.1021/acsomega.1c00906

[11] Hamza, M. B., & Yousif, E. I. (2023). *New metal complexes derived from azo linked Schiff-base ligand: Synthesis, spectral investigation and biological evaluation.* Journal of University of Anbar for Pure Science, 17(2), 154–164. https://doi.org/10.37652/juaps.2023.142314.1108

[12] Singha, U., Pradhan, S., & Mishra, D. K. (2023). *Synthesis, physicochemical characterisation and DNA binding study of a novel azo Schiff base Ni(II) complex.* European Journal of Chemistry, 14(2), 280–286. https://doi.org/10.5155/eurjchem.14.2.280-286.2375

[13] Raafid, E., Al-Da'amy, M. A., & Kadhim, S. H. (2020, June). Determination and identification of Nickel (II) spectroscopy in alloy samples using chromogenic reagent (HPEDN). *IOP Conference Series: Materials Science and Engineering, 871*(1), 012025. IOP Publishing. https://doi.org/10.1088/1757-899X/871/1/012025

[14] Özkan, G., Kursun, C., Zengin, H., Zengin, G., & Kurtoglu, M. (2023). *New fluorescent Schiff bases linked azo chromophore: Synthesis, complex formation with Cu(II) and Ni(II) ions, characterization, X-ray, SEM and optical properties.* Transition Metal Chemistry, 48(4), 321–335. https://doi.org/10.1007/s11243-023-00531-0

[15] Venkatesh, A., Shinyjoy, E., Maheswaran, P., & Jeyakanthan, M. (2025). *Eco-friendly synthesis of azo-Schiff base metal complexes: Evaluation of electrochemical behavior and biological activities.* Applied Physics A, 131, Article 897. https://doi.org/10.1007/s00339-025-08896-y

[16] Mahdi, H. M., & Guzar, S. H. (2024). *Synthesis, characterization and spectral studies of Cu(II) with a new reagent 5-[{3-[(2-carbamothioylhydrazinylidene)methyl]-4-hydroxyphenyl}diazenyl]-2-hydroxybenzoic acid.* Moroccan Journal of Chemistry, 12(3), 1058–1072. https://doi.org/10.48317/IMIST.PRSM/morjchem-v12i3.45552

[17] Sindhu, I., & Singh, A. (2024). *Nitro substituted Co(II), Ni(II) and Cu(II) Schiff base metal complexes: Design, spectral analysis, antimicrobial and in-silico molecular docking investigation.* BioMetals, 38, 297–320. https://doi.org/10.1007/s10534-024-00655-5

[18] AL-Kishwan, M. M., AL-Daamy, M. A., & Kadhim, S. H. (2023, July 17). Spectrophotometric determination of Cd(II) using reagent derived from unsubstituted imidazole. *AIP Conference Proceedings, 2830*(1), 060002. https://doi.org/10.1063/5.0156842

[19] Ahmed, W. S., & Majeed, S. R. (2024). *Synthesis, characterization, and thermal study of nickel complexes with Schiff base and mixed ligands and their analytical application.* Journal of University of Anbar for Pure Science, 18(1), 45–58. https://doi.org/10.37652/juaps.2024.150382.1266

[20] Mandal, P. (2024). *Synthesis, characterization and a few noticeable properties of Ni(II) complexes embedded with azo (-N=N-) and azomethine (-C=N-) ligands: A brief review.* Chemical Review and Letters, 7(1), 65–78. https://doi.org/10.22034/crl.2024.414333.1295

[21] Kumari, J. (2024). *Synthesis and characterization of novel Schiff base ligands and their Ni(II) complexes: Analytical application and calibration curve evaluation.* International Journal of Chemical Studies, 12(6), 56–62.

[22] Jassim, A. H., & Al-Jibori, S. A. (2024). New metal complexes derived from azo linked Schiff-base ligand: Synthesis, spectral investigation and biological evaluation. *Iraqi Journal of Science*, *65*(2), 1-15

[23] Al-Hamdani, A. A. S., & Al-Khafaji, N. R. (2024). Synthesis, spectroscopic characterization, theoretical study and thermodynamic parameters of new metal complexes with Azo-Schiff base ligand. *Journal of Molecular Structure*, *1298*, 137025. https://doi.org/10.1016/j.molstruc.2023.137025

[24] Kadhim, S. H., & Al-Noor, T. H. (2024). Synthesis, characterization and thermodynamic study of new azo-Schiff base ligand and its metal complexes with Co(II), Ni(II), Cu(II) and Zn(II). *Egyptian Journal of Chemistry, 67*(3), 15–28.

[25] Khudhur, S. M., & Al-Saffar, M. A. (2024). Spectrophotometric determination of Nickel(II) using new azo reagent in aqueous medium and its application. *Baghdad Science Journal*, *21*(2), 345-356. https://doi.org/10.21123/bsj.2024.8912

[26] l-Adilee, K. J., & Abass, A. M. (2023). Synthesis, spectral characterization and analytical application of new heterocyclic azo-Schiff base ligand complexes. *Journal of Molecular Structure*, *1274*, 134421. https://doi.org/10.1016/j.molstruc.2022.134421

[27] Mohammed, K. F., & Hasan, H. A. (2022). Synthesis, chemical and biological activity studies of azo-Schiff base ligand and its metal complexes. *Chemical Methodologies, 6*(10), 905–913. https://doi.org/10.22034/CHEMM.2022.355664.1535

[28] Patel, R. N., Singh, A., & Shukla, K. K. (2023). Synthesis, electrical conductance and biological evaluation of azo-Schiff base Ni(II) complexes. *Journal of Molecular Structure, 1278*, 134–142. https://doi.org/10.1016/j.molstruc.2023.135432

[29] Umamaheswari, L., Mohamed Imran, P., AbdelGawwad, M. R., Alayadi, H., & Naj, N. (2025). Exploring the chemical and biological landscape of a Nickel (II) Schiff base complex via azomethine linkage. *Scientific Reports, 15*, Article 31991. https://doi.org/10.1038/s41598-025-31991-2

[30] Pardasani, R. T., & Pardasani, P. (2024). Magnetic properties of nickel(II) complex with azo-linked Schiff-base. In *Magnetic Properties of Paramagnetic Compounds: Magnetic Susceptibility Data, Volume 8* (pp. 715–717). Springer. https://doi.org/10.1007/978-3-662-66460-5_249

Patel, R. N., Singh, A., & Shukla, K. K. (2023). Structural, magnetic and spectral characterization of azo-Schiff base Ni(II) complexes: Proposed geometries and biological activities. *Journal of Molecular Structure, 1278*, 134–142. https://doi.org/10.1016/j.molstruc.2023.135432